

Microstructures and Microsegregation of Directionally Solidified Mg-1.5Gd Magnesium Alloy with Different Growth Rates

Wang Jia'an¹, Wang Jiahe², Song Zhongxiao³

¹ China Huadian Electric Power Research Institute, Hangzhou 310030, China; ² State Key Laboratory of Solidification Processing, Northwestern Polytechnical University, Xi'an 710072, China; ³ Xi'an Jiaotong University, Xi'an 710049, China

Abstract: Directional solidification of Mg-1.5Gd (wt%) magnesium alloy was carried out to investigate the effects of the growth rate on the microstructures under controlled solidification conditions. A Bridgman-type directional solidification furnace with a liquid metal cooling (LMC) technique was used to solidify the specimens, which could provide steady state conditions with a constant temperature gradient (40 K/mm) at a wide range of growth rate (10–200 $\mu\text{m/s}$). Results show that the microstructures are cellular, and the relationship between cellular spacing (λ) and growth rate (V) is established in the form: $\lambda = 130.2827V^{0.2228}$ by a linear regression analysis, which is in good agreement with the calculated values by Trivedi model. The thermodynamics solidification path calculations by Scheil model and experimental observations confirm that the solidification microstructure in the alloy consists of primary $\alpha(\text{Mg})$ phase and binary eutectic $\alpha(\text{Mg})+\text{Mg}_5\text{Gd}$ phase. Meanwhile, the microsegregation of the alloying element predicted by the Scheil model agrees reasonably with the electron probe microanalysis (EPMA) measurements.

Key words: Mg-1.5Gd magnesium alloy; directional solidification; microstructures; cellular spacing; microsegregation

In view of their low density, high stiffness, high specific strength and excellent damping performance, magnesium alloys have a wide application prospect in the fields of aerospace, military industry, automobile, electronics etc.^[1]. Compared with aluminum alloys, however, the strength of magnesium alloys is still relatively low which limits their extensive application. To improve the mechanical properties of Mg alloys, Mg-RE (rare-earth elements, such as Gd, Y, Nd, etc.) alloys have been given tremendous attention due to their high specific strength at both room and elevated temperatures as well as their excellent creep resistance^[2-8]. Among them, Mg-Gd system is one of the promising candidates for a novel Mg-based heat-resistant alloy. Drits^[9], Rokhlin^[10] and Shigeharu^[11] et al. investigated the mechanical properties of Mg-Gd alloys with different mass fraction of Gd at different temperatures and found that the elevated temperature strength of Mg-20%Gd alloy is superior to that of the traditional WE54A heat-resistant magnesium alloys. Binary Mg-Gd alloys have also been reported to have a creep resistance superior to that of alloys WE43 and QE22 in terms of

steady-state creep rates^[12]. Meanwhile, a lot of researches have been developed about adding Sc, Y, Nd ect. rare-earth elements on the basis of Mg-Gd binary alloys, in order to decrease the density and costing and improve the mechanical properties^[2-8]. However, these researches mainly focus on the improvement of mechanical properties and there are few works reported on the solidification behavior of the Mg-Gd binary alloys under different casting conditions.

The objective of the present study is to investigate the microstructures and microsegregations of Mg-1.5Gd alloy and to establish the relationship between characteristic length scales and growth processing parameters quantitatively under controlled directional solidification conditions, which can enable us to predict the microstructure of this alloy system.

1 Experiment

Mg-1.5Gd alloy was prepared from pure Mg (99.98%) and Mg-28Gd (wt%) master alloy by melting in an electrical-resistance furnace under the protection of anti-oxidizing flux. The melts were poured into an iron test bar mould (preheated to

200~300 °C) at about 740 °C. Then, the test bars were further processed into the samples of $\Phi 7.8 \text{ mm} \times 90 \text{ mm}$ for subsequent directional solidification experiments.

A high temperature gradient Bridgman-type directional solidification furnace with a graphite heater and quenching system of water-cooled Ga-In-Sn liquid metals was used. The prepared sample ($\Phi 7.8 \text{ mm} \times 90 \text{ mm}$) was loaded in a special stainless tube crucible with 10 mm outer diameter (OD), 8 mm inner diameter (ID), 120 mm in length and sealed ends, which was designed to prevent the oxidation of the alloy^[13]. The crucible was put in the vacuum furnace with the graphite heater, pumped down to 1.1 Pa, backfilled with high-purity Ar₂ gas, and then heated to 800 °C for 30 min. When the axial temperature gradient reached 40 K/mm, the sample was directionally solidified by moving the crucible downward at a given speed (10~200 $\mu\text{m/s}$) for about 40 mm, and then quenched in Ga-In-Sn liquid metals. In the analysis, the withdrawal rate was approximately used as the growth rate.

For subsequent characterization, the solidified samples were cut along both the longitudinal and transverse sections to investigate the quenched interface morphology and the solidification microstructure. Olympus PM-G3 type optical microscope (OM) and JEOL JSM-5800 type scanning electron microscope (SEM) were used to examine the solidification microstructure. The phase analysis was conducted in an Oxford Inca type X-Ray energy dispersive spectroscope (EDS). The X-ray diffraction (XRD) was performed on a X'Pert PRO MPD type instrument in the diffraction angle (2θ) range between 20° and 90°, using Cu K α ($\lambda=0.154 \text{ nm}$) as a radiation source. The volume fraction of the second phase was measured by Image-Pro Plus 6.0 (Media Cybernetics, Inc., Bethesda, MD).

2 Results and Discussion

2.1 Phase diagram and solidification path calculation

Fig.1a shows the equilibrium phase diagram of the Mg-Gd binary system calculated by the thermodynamic calculation software Thermo-Calc^[14]. It can be seen that only $\alpha(\text{Mg})$ phase is formed during the cooling process in the equilibrium condition (the dash line in Fig.1a).

The calculated solidification path of Mg-1.5Gd alloy using Scheil model, which is based on the assumption of complete mixing in the liquid but no diffusion in the solid, is shown in Fig.1b. The sequence of phase formation is as follows: Liquid \rightarrow Liquid+ $\alpha(\text{Mg}) \rightarrow$ Liquid+ $\alpha(\text{Mg})+\text{Mg}_5\text{Gd} \rightarrow$ $\alpha(\text{Mg})+\text{Mg}_5\text{Gd}$. The ultimate phases consist of primary $\alpha(\text{Mg})$ phase and binary eutectic $\alpha(\text{Mg})+\text{Mg}_5\text{Gd}$ phase which is formed at 556 °C.

2.2 Phase identification

Fig.2 shows the XRD analysis results of the experimental alloy prepared by the directional solidification with various growth rates. It can be seen that only $\alpha(\text{Mg})$ phase and Mg_5Gd phase are found in the alloy, which is in good agreement with the calculated result of Scheil model. The SEM microstructures of the experimental alloy at growth rate of 10 $\mu\text{m/s}$ are given

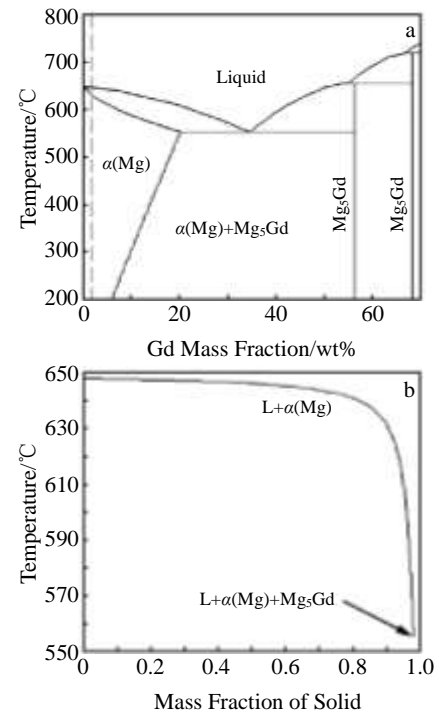


Fig.1 Equilibrium phase diagram of Mg-Gd binary system (a) and calculated solidification path of Mg-1.5Gd alloy using Scheil model (b)

in Fig.3a and 3b. It is noted that two portions are observed: the black portion presents typical cellular morphology and the white portion distributes along the grain boundary. The EDS results confirm that the black portion is $\alpha(\text{Mg})$ matrix phase and the white portion is $\alpha(\text{Mg})+\text{Mg}_5\text{Gd}$ binary eutectic phase, as shown in Fig.3c and 3d.

Meanwhile, the volume fractions of the eutectic phase were measured for the samples with different growth rates, shown in Table 1. The values calculated by Scheil model are also shown in the same table. It is found that the experimental values of eutectic phase fractions decrease with the increase of growth rate while that calculated by Scheil model are constant and the

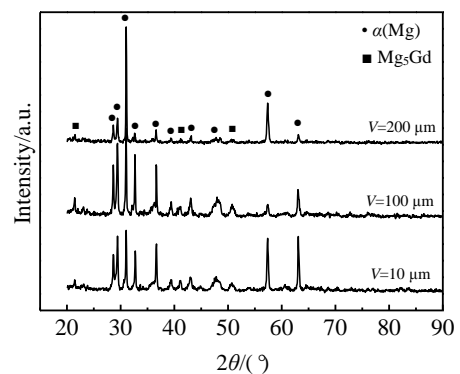


Fig.2 XRD patterns of the directional solidifying experimental alloy under $G=40 \text{ K/mm}$ at different growth rates

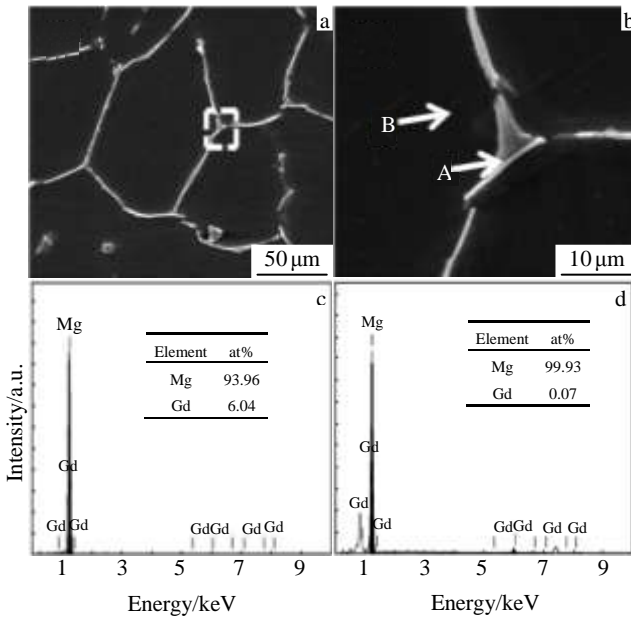


Fig.3 SEM images of the experimental alloy under $G=40$ K/mm at growth rate of $10 \mu\text{m/s}$ (a, b) and corresponding EDS results of point A (c), and point B (d) in Fig.3b

calculated values are higher than the experimentally measured values. This is mainly because the Scheil model ignores the back diffusion of alloying elements during the solidification.

2.3 Directional solidification microstructures

Optical microstructures of the directional solidifying Mg-1.5Gd alloy under the constant temperature gradient 40 K/mm at different growth rates are presented in Fig.4. It can be seen that $\alpha(\text{Mg})$ exhibits a typical cellular structure with coarse trunks along longitudinal section and regular cellular structure on transversal section.

It is well known that the cellular spacing has a significant effect on the mechanical properties such as yield strength and creep resistance of the alloy. Numerical models were proposed by Hunt^[15], Kurz and Fisher^[16] and Trivedi^[17] to characterize the cellular spacing under different solidification conditions as a function of C_0 , G and V , which are given by Eqs.(1)~(3) respectively:

$$\lambda = 2.83[m(k-1)D\Gamma]^{0.25} C_0^{0.25} V^{0.25} G^{-0.5} \quad (\text{Hunt model}) \quad (1)$$

$$\lambda = 4.3[m(k-1)D\Gamma/k^2]^{0.25} C_0^{0.25} V^{0.25} G^{-0.5} \quad (\text{Kurz-Fisher model}) \quad (2)$$

$$\lambda = 2.83[m(k-1)D\Gamma L]^{0.25} C_0^{0.25} V^{0.25} G^{-0.5} \quad (\text{Trivedi model}) \quad (3)$$

where, Γ is the Gibbs-Thomson coefficient, m is the liquids line slope, k is the partition coefficient, C_0 is the initial alloy composition, D is the diffusion coefficient in the liquid, L is a constant with the value of 28 that depends on harmonic perturbations. Thermophysical parameters of Mg-1.5Gd alloy used in calculations for the models are given in Table 2.

The experimental values of cellular spacing of the experimental alloy are shown in Table 3. It can be seen that the cellular spacing λ decreases with the increase of growth rate V .

Table 1 Experimental measured and thermodynamically calculated volume fractions of the eutectic phase in Mg-1.5Gd alloy

Growth rate, $V/\mu\text{m s}^{-1}$	Eutectic volume fraction/vol%	
	Image analysis results	Calculation results by Scheil model
10	1.06	1.19
40	1.01	1.19
100	0.89	1.19
200	0.73	1.19

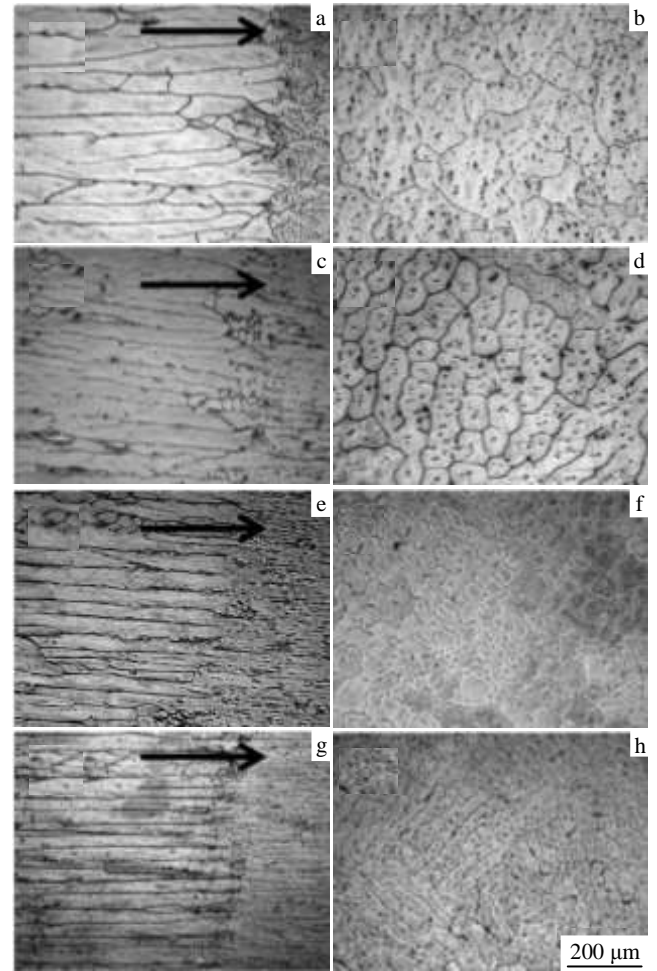


Fig.4 OM microstructures of the directional solidifying experimental alloy under $G=40$ K/mm at different growth rate: (a, b) $10 \mu\text{m/s}$, (c, d) $60 \mu\text{m/s}$, (e, f) $150 \mu\text{m/s}$, and (g, h) $200 \mu\text{m/s}$

Table 2 Thermophysical parameters of Mg-1.5Gd alloy

Parameter	Symbol	Unit	Value	Ref.
Initial composition	C_0	wt%	1.5	
Slope of liquid line	m	K/wt%	-1.274	
Distribution coefficient	k	-	0.0993	
Diffusion coefficient (Liquid)	D	cm^2/s	1.233×10^{-9}	[18]
Gibbs-Thomson coefficient	Γ	m K	1.1×10^{-7}	[18]

Table 3 Experimental and calculated values of cellular spacing of Mg-1.5Gd alloy

$V/\mu\text{m s}^{-1}$	$\lambda/\mu\text{m}$ (Exp.)	$\lambda/\mu\text{m}$ (Hunt)	$\lambda/\mu\text{m}$ (Kurz-Fisher)	$\lambda/\mu\text{m}$ (Trivedi)
10	77.09	31.10	149.97	71.54
40	55.65	21.99	106.05	50.59
60	52.13	19.87	95.82	45.71
100	45.33	17.49	84.36	40.23
150	40.37	15.81	76.23	36.36
200	35.38	14.71	70.90	33.83

The data from Table 3 are plotted in Fig.5. It can be seen that the relationship between $\log\lambda$ and $\log V$ are essentially linear for the growth velocity. Through linear regression analysis, the relationship between λ and V under the temperature gradient of 40 K/mm was established as follows:

$$\lambda = 130.2827V^{-0.2228} \quad (4)$$

In additional, the values of cellular spacing calculated by the Hunt model, the Kurz-Fisher model, and the Trivedi model are also given in Fig.5. It can be seen that the values calculated by Kurz-Fisher model and Hunt model obviously diverge from the measured results, while the measured results are in good agreement with the values calculated by Trivedi model. However, we can not ignore that there still exist a little of deviations between the calculations and the experimental results, since the directional solidification was carried out on the stainless tube crucible with lower thermal conductivity (0.16 W/cm K) compared with that of pure magnesium melt (1.56 W/cm K)^[15]. Thus the stainless pipe wall may obstruct the heat spreading and coarsen the trunk of the cellular spacing. Meanwhile, some experimental errors, such as, solidification parameter errors and spacing measurement errors may also cause the deviation of experimental results from the prediction of theories models.

2.4 Microsegregation

Microsegregation has a significant effect on the properties of the alloys, such as the inhomogeneous precipitation, fatigue behavior and corrosion resistance^[19]. Fig.6 shows the BSE images and the EPMA maps of Mg and Gd elements in the Mg-1.5Gd alloy prepared from samples with the growth rate of 30 and 200 $\mu\text{m/s}$. It can be seen that most of Gd element are concentrated along the grain boundary formed at the end of solidification while Mg is mainly distributed in the grain interior.

Fig.7 shows the measured concentration profile of Gd as a function of solid fraction at the growth rates of 10, 100 and 200 $\mu\text{m/s}$. It reveals that the Gd content increases gradually as the solidification proceeds but increases abruptly at the formation of the Mg_5Gd phase. As shown in the same figure, the concentration profile of Gd was also calculated using Scheil model. It is noted that the measured concentration profile of Gd for three growth rates agree reasonably with the calculation one.

It is also noted that such agreement is connected with the growth rate. The measured concentration profile of Gd for the growth rate of 200 $\mu\text{m/s}$ agrees better with the calculation one than that for the growth rates of 10 and 100 $\mu\text{m/s}$. This is due to the influence of back-diffusion of alloying element decreasing with the increase of growth rate while in Scheil model back-diffusion is ignored. Thus, it is indicated that the microsegregation of alloying element Gd in the Mg-1.5Gd alloy prepared by directional solidification can be described by Scheil model with accuracy.

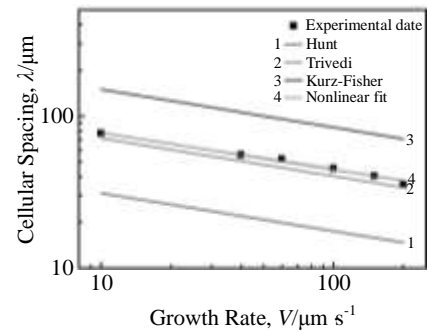


Fig.5 Comparison of observed cellular spacing with the predictions of different theory models

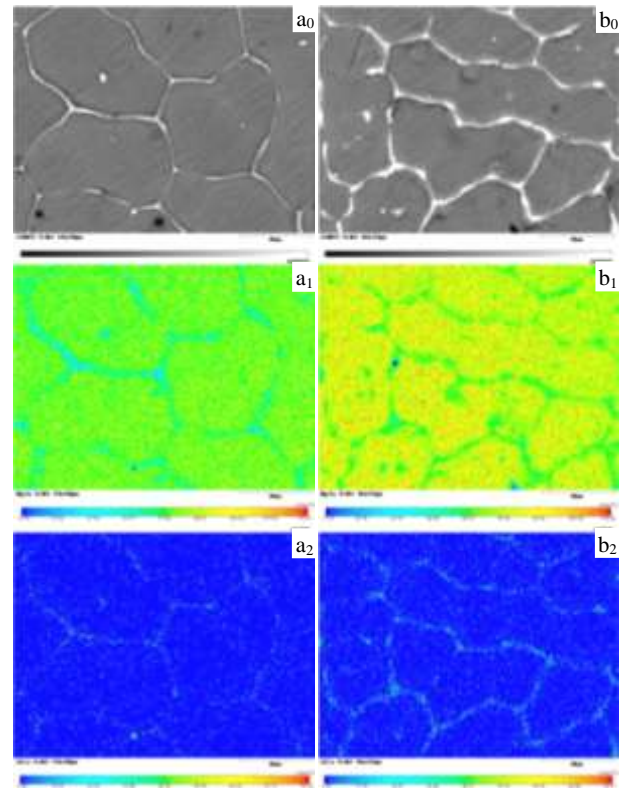


Fig.6 EPMA backscatter images (a_0 , b_0) and Mg (a_1 , b_1), Gd (a_2 , b_2) distribution maps of the directional solidifying experimental alloy under $G=40$ K/mm at 30 $\mu\text{m/s}$ (a) and 200 $\mu\text{m/s}$ (b)

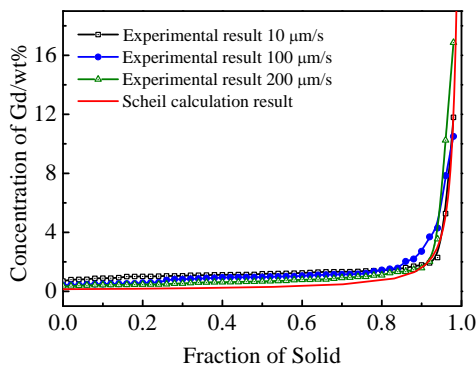


Fig.7 Microsegregation of Gd in the directional solidifying experimental alloy under $G=40$ K/mm at different growth rates

3 Conclusions

1) The directionally solidified Mg-1.5Gd alloy is mainly consisted of primary $\alpha(\text{Mg})$ phase and $\alpha(\text{Mg})+\text{Mg}_5\text{Gd}$ binary eutectic phase, which agrees well with the prediction of Scheil model.

2) The primary $\alpha(\text{Mg})$ phase exhibits a typical cellular structure and the cellular spacing λ can be expressed as a function of growth rate V in the form: $\lambda=130.2827V^{0.2228}$ by a linear regression analysis under a constant temperature gradient (40 K/mm) at the growth rate between 10~200 $\mu\text{m/s}$.

3) The experimental cellular spacing values are in good agreement with the cellular spacing values calculated by Trivedi model but largely diverge from that calculated by Hunt model and Kurz-Fisher model.

4) The microsegregation of Gd in the directionally solidified Mg-1.5Gd alloy measured by EPMA agrees reasonably with the results predicted by the Scheil model, suggesting that the Scheil model can be used for predicting the microsegregation of cast magnesium alloys.

References

- 1 Yang Z, Li J P, Zhang J X et al. *Acta Metall Sin, Engl Lett*[J], 2008, 21(5): 313
- 2 Wang J, Meng J, Zhang D P et al. *Mater Sci Eng A*[J], 2007, 456: 78
- 3 Gao L, Chen R S, Han E H. *J Alloy Compd*[J], 2009, 481: 379
- 4 Nie J F, Gao X, Zhu S M. *Scripta Materialia*[J], 2005, 53: 1049
- 5 Michiaki Y, Tsutomu A, Shintaro Y et al. *Scripta Materialia*[J], 2005, 53: 799
- 6 Ifeanyi A A, Shigeharu K, Yo K. *Mater Trans*[J], 2001, 42(7): 1212
- 7 Yi Jianlong, Zhang Xinming, Ma Guang et al. *Rare Metal Materials and Engineering*[J], 2009, 38(10): 1852 (in Chinese)
- 8 Wang Ping, Liu Daoxin, Li Jianping et al. *Rare Metal Materials and Engineering*[J], 2011, 40(6): 995 (in Chinese)
- 9 Drits M E, Sviderkaya Z A, Rokhlin L L et al. *Metallovedenie Termicheskaya Obrabotka Metallov*[J], 1979, 11: 62
- 10 Rokhlin L L, Nikitina N I. *Fizika Metallov Metallovedenie*[J], 1986, 62(4): 781
- 11 Shigeharu K, Shigeru I, Kiyooki O et al. *Journal of Japan Institute of Light Metals*[J], 1992, 42(12): 727
- 12 Mordike B L. *Mater Sci Eng A*[J], 2002, A324: 103
- 13 Liu S J. *China Patent*, 201310014615.5[P]. 2013
- 14 Andersson J O, Helander T, Höglund L et al. *Thermo-Calc and DICTRA, Computational Tools for Materials Science*[M]. Calphad, 2002, 26: 273
- 15 Hunt J D. *Solidification and Casting of Metals*[M]. London: The Metal Society, 1979: 3
- 16 Kurz W, Fisher D J. *Acta Metall*[J], 1981, 29: 11
- 17 Trivedi R. *Metall Trans A*[J], 1984, 15: 977
- 18 Kurz W, Fisher D J. *Fundamentals of Solidification*[M]. Switzerland: Trans Tech Publications, 1998
- 19 Zhang C, Ma D, Wu K S et al. *Science Direct Intermetallics*[J], 2007, 15: 1395

不同速率定向凝固条件 Mg-1.5Gd 镁合金的微观结构及微观偏析

王甲安¹, 王甲贺², 宋忠孝³

(1. 华电电力科学研究院, 浙江 杭州 310030)

(2. 西北工业大学 凝固技术国家重点实验室, 陕西 西安 710072)

(3. 西安交通大学, 陕西 西安 710049)

摘要: 研究了在定向凝固条件下凝固速率对 Mg-1.5Gd 镁合金微观结构的影响。试样通过 Bridgman 定向凝固炉来制备, 温度梯度恒定为 40 K/mm, 凝固速率为 10~200 $\mu\text{m/s}$ 。研究发现, Mg-1.5Gd 镁合金凝固组织为典型胞晶结构, 通过线性拟合得到胞晶间距(λ)与凝固速率(V)关系为: $\lambda=130.2827V^{0.2228}$, 此结论与 Trivedi 模型拟合较好。通过 Scheil 模型进行热力学凝固路径计算, 结合试验观察可以确定凝固组织为 $\alpha(\text{Mg})$ 相和 $\alpha(\text{Mg})+\text{Mg}_5\text{Gd}$ 二元共晶相。同时, 通过 Scheil 模型计算所得的 Gd 元素的微观偏析与 EPMA 测量结果基本一致。

关键词: Mg-1.5Gd 二元合金; 定向凝固; 微观结构; 胞晶间距; 微观偏析